Supplementary Information

Vibrational spectroscopy coupled with machine learning sheds light on the cellular effects induced by rationally designed TLR4 agonists

Diletta Ami[a,1], Ana Rita Franco[a,1], Valentina Artusa[a], Alessio Romerio[a], Mohammed Monsoor Shaik[a], Alice Italia[a], Juan Anguita[b,c], Samuel Pasco[b], Paolo Mereghetti[d], Francesco Peri[a*], Antonino Natalello[a*]

[a] *Department of Biotechnology and Biosciences, University of Milano-Bicocca; Piazza della Scienza, 2; 20126 Milano (Italy)*

[b] *Center for Cooperative Research in Biosciences (CIC bioGUNE), Basque Research and Technology Alliance (BRTA), 48160 Derio, Bizkaia, Spain.*

[c] *Ikerbasque, Basque Foundation for Science, Plaza Euskadi 5, 48009 Bilbao, Bizkaia, Spain.*

[d] *Bioinformatics Consultant, 15061 Arquata Scrivia, Italy.*

[1] These Authors contributed equally

*Corresponding Authors: Francesco Peri, francesco.peri@unimib.it; Antonino Natalello, antonino.natalello@unimib.it

Table of Contents

1. Supplementary Figures and Tables

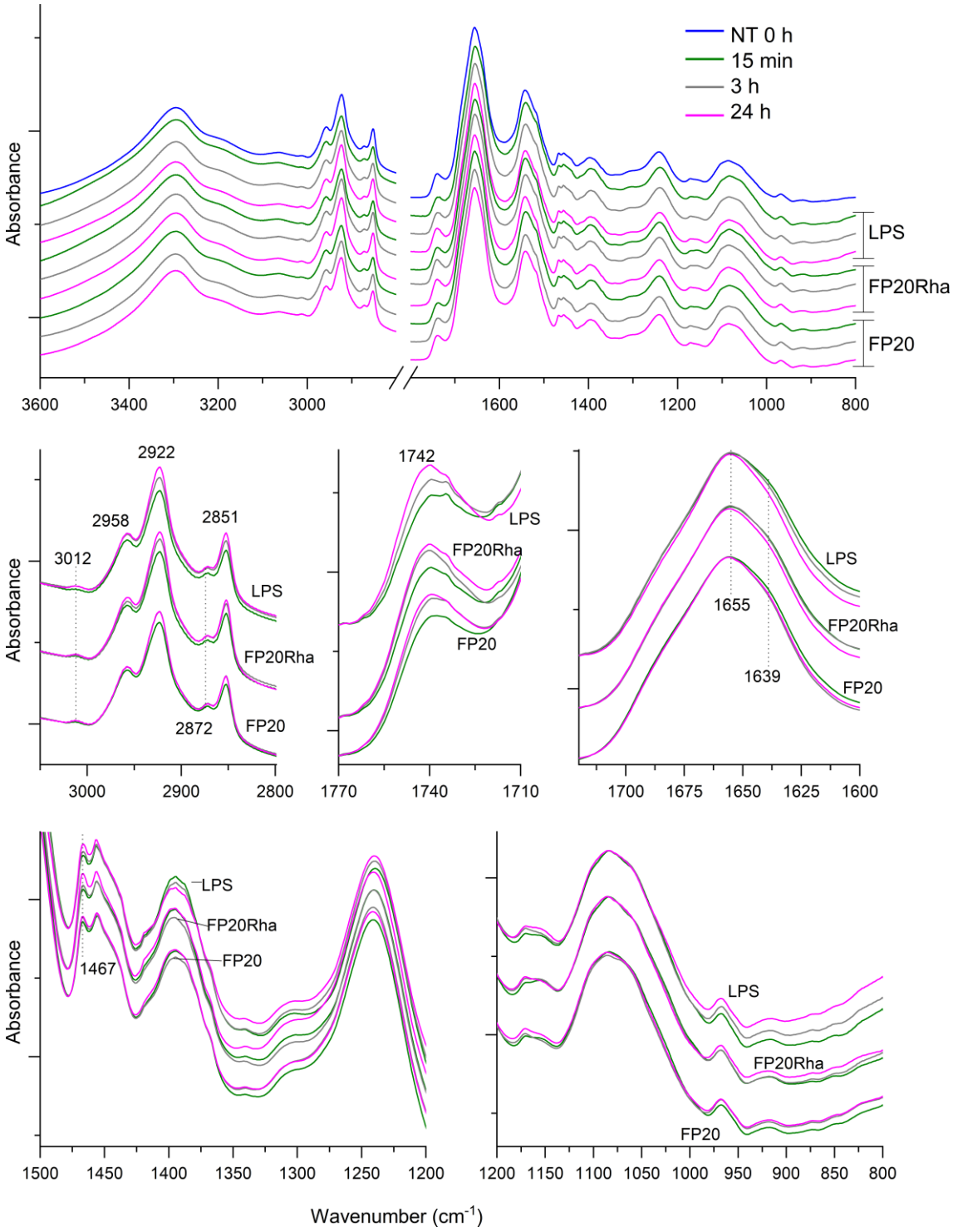

Figure S1. Mean absorption FTIR spectra for each experimental group. Mean absorption FTIR spectra of human TDM cells not treated (NT 0 h) and treated with different TLR4 agonists at different time points (15 min, 3 h, 24 h). Spectra were reported in the whole measured range or in selected spectral regions. The average absorption spectra are reported after normalization at the Amide I band area of the measured spectra and have been offset for the clarity of the figures.

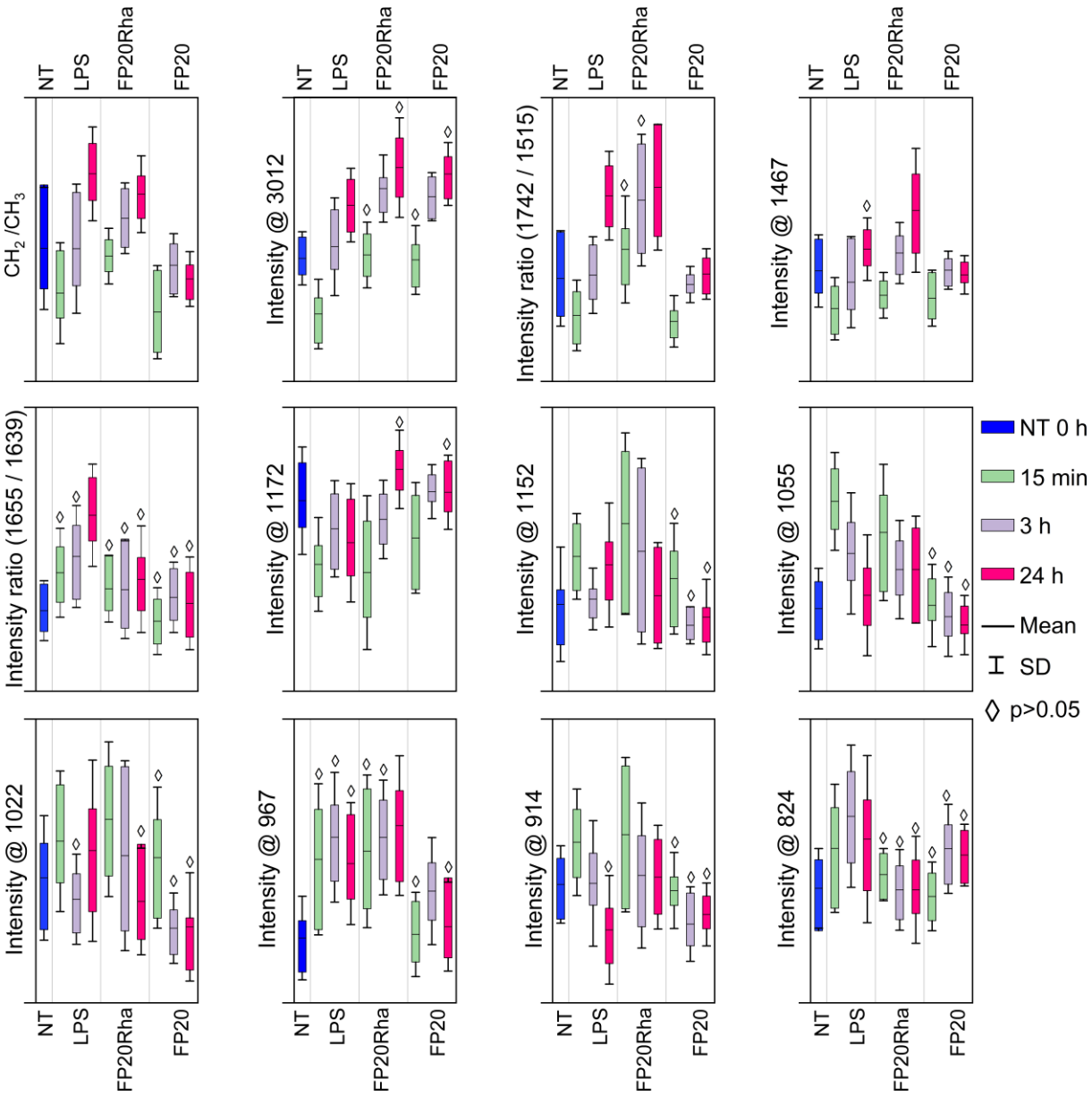

Figure S2. Box plots (25/75th percentiles) of the intensity and of the intensity ratio of the most relevant peaks in the FTIR analysis of TDM cells treated with different TLR4 agonists. Peak intensities are taken from inverted second derivatives. Statistical significance has been computed using t-tests, taking as reference not treated (NT) cells at 0 h. P-values were computed with Holm correction (see Table S1 for more details of the statistical analysis).

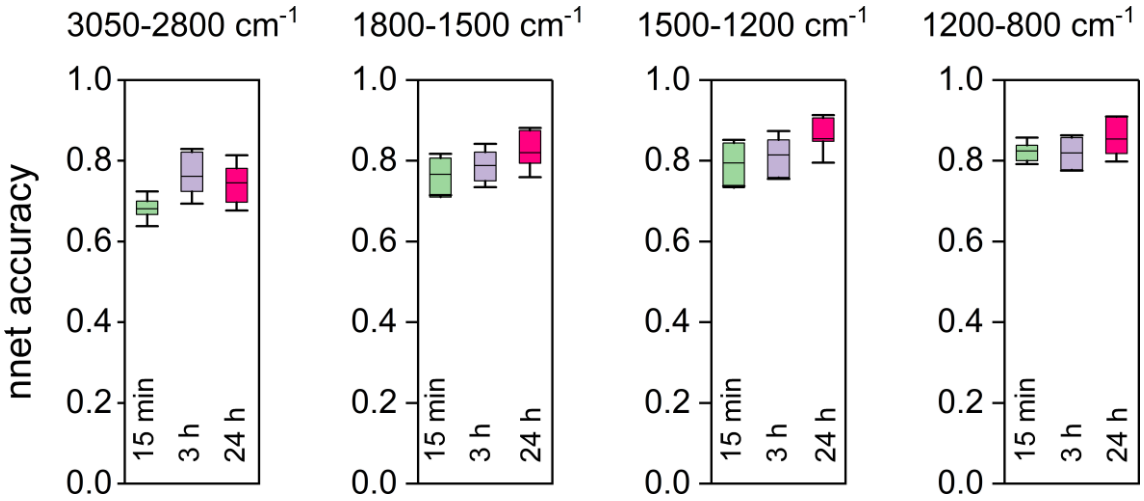

Figure S3. Overall nnet discrimination accuracy for the analysis performed in different spectral ranges. Box plots (25/75th percentiles), mean lines, and standard deviations are reported. The treatment times are indicated.

Table S1 - a. MANOVA results			
Source of variation	**Dfs**	**F-value**	**P-value**
CH_2 / CH_3			
treatment	3	30.50	1.22E-17
time	3	45.80	3.42E-25
treatment:time	6	17.29	1.20E-17
treatment:time: Linear	1	60.87	6.29E-14
treatment:time: Quadratic	1	16.36	6.37E-05
treatment:time: Cubic	1	11.33	8.41E-04
1655 / 1639			
treatment	3	39.85	2.46E-22
time	3	8.24	2.53E-05
treatment:time	6	4.18	4.43E-04
treatment:time: Linear	1	18.34	2.36E-05
treatment:time: Quadratic	1	0.09	7.67E-01
treatment:time: Cubic	1	1.90	1.69E-01
1742/1515			
treatment	3	46.73	1.25E-25
time	3	64.23	1.88E-33
treatment:time	6	14.42	8.62E-15
treatment:time: Linear	1	50.02	7.64E-12
treatment:time: Quadratic	1	7.93	5.12E-03
treatment:time: Cubic	1	7.44	6.69E-03
Response i_1467			
treatment	3	23.99	3.28E-14
time	3	44.55	1.34E-24
treatment:time	6	8.02	3.79E-08
treatment:time: Linear	1	3.28	7.08E-02
treatment:time: Quadratic	1	36.00	4.71E-09
treatment:time: Cubic	1	2.52	1.13E-01

Response i_1022			
treatment	3	18.16	5.16E-11
time	3	18.80	2.26E-11
treatment:time	6	3.95	7.67E-04
treatment:time: Linear	1	9.92	1.77E-03
treatment:time: Quadratic	1	2.23	1.36E-01
treatment:time: Cubic	1	1.78	1.82E-01
Response i_3012			
treatment	3	42.77	9.47E-24
time	3	144.65	5.05E-62
treatment:time	6	3.19	4.60E-03
treatment:time: Linear	1	7.47	6.58E-03
treatment:time: Quadratic	1	0.79	3.76E-01
treatment:time: Cubic	1	1.22	2.70E-01
Response i_1172			
treatment	3	38.82	7.81E-22
time	3	21.59	6.56E-13
treatment:time	6	6.28	2.68E-06
treatment:time: Linear	1	6.33	1.23E-02
treatment:time: Quadratic	1	23.59	1.76E-06
treatment:time: Cubic	1	4.83	2.86E-02
Response i_1055			
treatment	3	48.41	2.06E-26
time	3	21.35	8.97E-13
treatment:time	6	4.93	7.28E-05
treatment:time: Linear	1	26.18	5.01E-07
treatment:time: Quadratic	1	1.56	2.12E-01
treatment:time: Cubic	1	0.11	7.42E-01
Response i_1152			
treatment	3	28.49	1.35E-16

time	3	11.03	5.95E-07
treatment:time	6	3.99	6.91E-04
treatment:time: Linear	1	5.63	1.82E-02
treatment:time: Quadratic	1	7.62	6.07E-03
treatment:time: Cubic	1	1.97	1.62E-01
Response i_967			
treatment	3	28.86	8.62E-17
time	3	10.12	2.01E-06
treatment:time	6	1.65	1.33E-01
treatment:time: Linear	1	0.92	3.37E-01
treatment:time: Quadratic	1	1.16	2.83E-01
treatment:time: Cubic	1	0.19	6.67E-01
Response i_914			
treatment	3	17.37	1.43E-10
time	3	29.67	3.29E-17
treatment:time	6	3.04	6.55E-03
treatment:time: Linear	1	13.93	2.19E-04
treatment:time: Quadratic	1	0.38	5.39E-01
treatment:time: Cubic	1	0.31	5.77E-01
Response i_824			
treatment	3	22.95	1.21E-13
time	3	2.96	3.24E-02
treatment:time	6	2.09	5.31E-02
treatment:time: Linear	1	0.05	8.22E-01
treatment:time: Quadratic	1	6.50	1.12E-02
treatment:time: Cubic	1	0.63	4.26E-01

Table S1 - b. Post-hoc pairwise T-tests results

Pair	Time	Variable	Number of measurements NT	Number of measurements treatment	T-value	P-value
NT-LPS	15 min	CH_2 / CH_3	14	47	-7.21	4.11E-10
NT-FP20Rha	15 min	CH_2 / CH_3	14	29	-4.04	2.97E-04
NT-FP20	15 min	CH_2 / CH_3	14	22	-7.73	3.48E-11
NT-LPS	3h	CH_2 / CH_3	16	41	-5.09	8.32E-06
NT-FP20Rha	3h	CH_2 / CH_3	16	27	-2.72	2.32E-02
NT-FP20	3h	CH_2 / CH_3	16	20	-5.51	1.66E-06
NT-LPS	24h	CH_2 / CH_3	37	47	5.94	1.04E-07
NT-FP20Rha	24h	CH_2 / CH_3	37	30	3.22	3.29E-03
NT-FP20	24h	CH_2 / CH_3	37	17	-4.62	2.75E-05
NT-LPS	15 min	1655 / 1639	14	47	1.87	2.55E-01
NT-FP20Rha	15 min	1655 / 1639	14	29	0.53	5.95E-01
NT-FP20	15 min	1655 / 1639	14	22	-1.85	2.55E-01
NT-LPS	3h	1655 / 1639	16	41	2.20	1.20E-01
NT-FP20Rha	3h	1655 / 1639	16	27	-0.24	1.00E+00
NT-FP20	3h	1655 / 1639	16	20	-0.73	1.00E+00
NT-LPS	24h	1655 / 1639	37	47	7.80	1.16E-11
NT-FP20Rha	24h	1655 / 1639	37	30	1.72	2.66E-01
NT-FP20	24h	1655 / 1639	37	17	-0.22	8.22E-01
NT-LPS	15 min	1742/1515	14	47	-6.72	3.60E-09
NT-FP20Rha	15 min	1742/1515	14	29	-0.89	7.48E-01
NT-FP20	15 min	1742/1515	14	22	-6.44	1.00E-08
NT-LPS	3h	1742/1515	16	41	-6.31	3.88E-08
NT-FP20Rha	3h	1742/1515	16	27	-0.66	9.03E-01
NT-FP20	3h	1742/1515	16	20	-6.16	4.63E-08
NT-LPS	24h	1742/1515	37	47	3.80	6.81E-04
NT-FP20Rha	24h	1742/1515	37	30	4.15	2.43E-04
NT-FP20	24h	1742/1515	37	17	-3.04	5.68E-03
NT-LPS	15 min	i_1467	14	47	7.97	1.06E-11
NT-FP20Rha	15 min	i_1467	14	29	5.95	1.48E-07
NT-FP20	15 min	i_1467	14	22	5.98	1.48E-07
NT-LPS	3h	i_1467	16	41	6.34	4.07E-08
NT-FP20Rha	3h	i_1467	16	27	3.29	4.59E-03

NT-FP20	3h	i_1467	16	20	4.56	7.36E-05
NT-LPS	24h	i_1467	37	47	1.11	2.69E-01
NT-FP20Rha	24h	i_1467	37	30	-2.70	2.35E-02
NT-FP20	24h	i_1467	37	17	2.87	1.90E-02
NT-LPS	15 min	i_1022	14	47	-3.35	5.55E-03
NT-FP20Rha	15 min	i_1022	14	29	-4.12	4.40E-04
NT-FP20	15 min	i_1022	14	22	-2.28	9.71E-02
NT-LPS	3h	i_1022	16	41	-2.35	6.20E-02
NT-FP20Rha	3h	i_1022	16	27	-4.52	1.02E-04
NT-FP20	3h	i_1022	16	20	-0.62	5.39E-01
NT-LPS	24h	i_1022	37	47	-6.17	4.98E-08
NT-FP20Rha	24h	i_1022	37	30	-2.36	5.98E-02
NT-FP20	24h	i_1022	37	17	-0.64	5.21E-01
NT-LPS	15 min	i_1172	14	47	5.63	7.18E-07
NT-FP20Rha	15 min	i_1172	14	29	5.72	5.87E-07
NT-FP20	15 min	i_1172	14	22	3.64	1.68E-03
NT-LPS	3h	i_1172	16	41	7.20	6.69E-10
NT-FP20Rha	3h	i_1172	16	27	6.00	1.60E-07
NT-FP20	3h	i_1172	16	20	3.60	2.01E-03
NT-LPS	24h	i_1172	37	47	6.69	3.80E-09
NT-FP20Rha	24h	i_1172	37	30	0.03	9.74E-01
NT-FP20	24h	i_1172	37	17	1.59	3.44E-01
NT-LPS	15 min	i_3012	14	47	6.38	2.22E-08
NT-FP20Rha	15 min	i_3012	14	29	0.54	1.00E+00
NT-FP20	15 min	i_3012	14	22	0.95	1.00E+00
NT-LPS	3h	i_3012	16	41	7.42	2.33E-10
NT-FP20Rha	3h	i_3012	16	27	2.44	3.32E-02
NT-FP20	3h	i_3012	16	20	2.88	1.47E-02
NT-LPS	24h	i_3012	37	47	3.18	9.21E-03
NT-FP20Rha	24h	i_3012	37	30	-0.65	1.00E+00
NT-FP20	24h	i_3012	37	17	-0.04	1.00E+00
NT-LPS	15 min	i_1055	14	47	-7.31	2.42E-10
NT-FP20Rha	15 min	i_1055	14	29	-4.98	8.01E-06
NT-FP20	15 min	i_1055	14	22	-0.59	5.59E-01

NT-LPS	3h	i_1055	16	41	-4.02	5.57E-04
NT-FP20Rha	3h	i_1055	16	27	-2.79	1.91E-02
NT-FP20	3h	i_1055	16	20	0.05	9.57E-01
NT-LPS	24h	i_1055	37	47	-2.59	4.33E-02
NT-FP20Rha	24h	i_1055	37	30	-4.33	1.83E-04
NT-FP20	24h	i_1055	37	17	0.02	9.81E-01
NT-LPS	15 min	i_1152	14	47	-3.75	1.44E-03
NT-FP20Rha	15 min	i_1152	14	29	-5.18	6.32E-06
NT-FP20	15 min	i_1152	14	22	-2.26	7.01E-02
NT-LPS	3h	i_1152	16	41	-2.75	2.10E-02
NT-FP20Rha	3h	i_1152	16	27	-5.47	2.02E-06
NT-FP20	3h	i_1152	16	20	-0.91	3.63E-01
NT-LPS	24h	i_1152	37	47	-6.01	1.12E-07
NT-FP20Rha	24h	i_1152	37	30	-2.80	2.34E-02
NT-FP20	24h	i_1152	37	17	-0.84	4.03E-01
NT-LPS	15 min	i_967	14	47	-2.18	9.32E-02
NT-FP20Rha	15 min	i_967	14	29	-2.41	7.02E-02
NT-FP20	15 min	i_967	14	22	1.35	3.57E-01
NT-LPS	3h	i_967	16	41	0.12	1.00E+00
NT-FP20Rha	3h	i_967	16	27	0.13	1.00E+00
NT-FP20	3h	i_967	16	20	2.68	3.47E-02
NT-LPS	24h	i_967	37	47	-2.22	6.25E-02
NT-FP20Rha	24h	i_967	37	30	-4.21	2.41E-04
NT-FP20	24h	i_967	37	17	1.43	1.56E-01
NT-LPS	15 min	i_914	14	47	-3.04	8.82E-03
NT-FP20Rha	15 min	i_914	14	29	-3.26	5.94E-03
NT-FP20	15 min	i_914	14	22	-0.19	1.00E+00
NT-LPS	3h	i_914	16	41	-3.12	1.19E-02
NT-FP20Rha	3h	i_914	16	27	-3.35	6.93E-03
NT-FP20	3h	i_914	16	20	-0.66	1.00E+00
NT-LPS	24h	i_914	37	47	-0.49	6.24E-01
NT-FP20Rha	24h	i_914	37	30	-5.20	4.73E-06
NT-FP20	24h	i_914	37	17	-1.53	3.84E-01
NT-LPS	15 min	i_824	14	47	-3.92	8.72E-04

NT-FP20Rha	15 min	i_824	14	29	-1.96	1.58E-01
NT-FP20	15 min	i_824	14	22	-0.52	6.06E-01
NT-LPS	3h	i_824	16	41	-3.88	9.33E-04
NT-FP20Rha	3h	i_824	16	27	0.68	5.00E-01
NT-FP20	3h	i_824	16	20	-1.62	2.16E-01
NT-LPS	24h	i_824	37	47	-3.14	1.06E-02
NT-FP20Rha	24h	i_824	37	30	0.52	7.34E-01
NT-FP20	24h	i_824	37	17	-1.48	4.26E-01

Table S1. Detailed results of MANOVA analysis (a) and post-hoc pairwise T-test analysis (b).
a) MANOVA was applied as described in Methods. Results are grouped by each different response variable. The first column shows the source of variation. As a source of variation, the treatment, time and their interaction were considered. Moreover, the trend was also analysed using linear, quadratic and cubic contrasts. The second column (Dfs) shows the degrees of freedom of the given factor. The third column indicates the result of the F-statistic and the last column is the associated P-value.
b) Post-hoc pairwise T-tests have been performed as described in Methods. For a given variable at a given time, multiple pairwise T-tests have been computed between the NT and the treated group. The numerosity of the NT and of the treated group is shown in columns “Number of measurements NT” and “Number of measurements treated”, respectively. The last two columns show the value of the T-test and its associated P-value.

Peak positions (cm^{-1})	Assignment	References
~3012	Olefinic =CH stretching	[1]
~2958	CH_3 asymmetric stretching	[1,2]
~2922	CH_2 antisymmetric stretching	[1,2]
~2872	CH_3 symmetric stretching	[1,2]
~2851	CH_2 symmetric stretching	[1,2]
~1742	C=O stretching from lipid ester groups	[1]
~1655	C=O stretching, Amide I band, α-helices/random coils	[2,3]
~1639	C=O stretching, Amide I band, β-sheets	[2,3]
~1467	CH_2 and CH_3 bending, mainly from lipid hydrocarbon chains	[1,2]
~1172	CO-O-C stretching in lipids; carbohydrates: C-OH, C-C stretching and C-O-H bending; SO_4, C-O-S stretching mainly from GAGs; non-hydrogen-bonded C-O of the C-OH groups of serine, threonine and tyrosine residues	[1,2,4–9]
~1152	Carbohydrates: ring vibrations overlapped with stretching vibrations of (C-OH) side groups and the (C-O-C) glycosidic bond vibration; SO_4, C-O-S stretching mainly from GAGs; hydrogen-bonded C-O of the C-OH groups of serine, threonine and tyrosine residues	[5–9]
~1055	Polysaccharide ring and side group vibrations and GAG vibrations	[5,6,10,11]
~1022	Polysaccharide ring and side group vibrations and GAG vibrations	[5,6,10,11]
~967	$N(CH_3)_3$ asymmetric stretching of PC and SM; C-C stretching of DNA backbone; RNA ribose-phosphate main chain vibrations	[1,2,12]
~914	Polysaccharide ring vibrations and GAG vibrations	[5,7]
~838-805	Glycosidic linkages of polysaccharides, sulfated GAG vibrations	[5,13–15]

Table S2. Assignment of the relevant IR components. The peak positions from second derivative spectra have been reported for the spectral components discussed in the text. The main assignment to the cell biomolecules has been indicated.

2. Supplementary Methods

2.1. Cell cultures

HEK Blue cells (InvivoGen) were cultured in Dulbecco's modified Eagle's medium (DMEM) high glucose supplemented with 10% heat-inactivated fetal bovine serum (FBS), 2 mM L-glutamine, and 100 U/mL of Penicillin-Streptomycin at 37 °C, 5% CO_2, 95% humidity. Cells were subcultured every other day. THP-1 X-Blue cells (InvivoGen) were cultured in RPMI 1640, 10% heat-inactivated FBS, 2 mM L-glutamine, and 100 U/mL of Penicillin-Streptomycin and maintained at 37 °C, 5% CO_2, 95% humidity. Cells were kept at a density of 0.5×10^6 cells/mL. Media and supplements were purchased from Euroclone.

2.2. Cell Treatments for HEK-Blue hTLR4 and hTLR2 SEAP Cell Reporter Assay

HEK Blue cells were seeded 3 x 10^4 cells/well in 96-well plates. Cells were treated with increasing concentrations of FP20 and FP20Rha (0.1 - 25 μM), 10 ng/mL of Pam2CysSerLys4 (PAM2CSK4) (Invivogen) and 100 ng/mL of Smooth-LPS(S-LPS) from *S. minn* (Innaxon). After 16 to 18 hours of incubation, supernatant was collected.

2.3. Cell Treatments for THP-1 X-Blue Cell Reporter Assay and Cytokine Detection

THP-1 X-Blue cells were seeded using 180 μL of a 4 x 10^5 cells/mL cell suspension in 96-well plates. THP-1 X-Blue cells were differentiated into TDMs by exposure to 100 ng/mL of phorbol 12-myristate 13-acetate (PMA, Invivogen). After 72 hours of incubation, medium was removed and replaced with PMA-free RPMI medium. Cells were then treated with increasing concentrations of FP20 and FP20Rha (0.1 - 10 μM) for cell reporter assays or with 10 μM of the compounds for cytokine detection experiments. S-LPS 100 ng/mL and MPLA 1 μg/mL from *S. minn* (Innaxon) were used as positive controls for cell reporter assays while S-LPS 100 ng/mL was used for comparability purposes for cytokine detection experiments.

2.4. Secreted Embryonic Alkaline Phosphatase Cell Reporter Assay

HEK-Blue and TDM were treated with the above mentioned concentrations of FP20, FP20Rha, S-LPS or MPLA. After 16 to 18 hours of incubation, supernatant was collected and Secreted Embryonic Alkaline Phosphatase (SEAP) levels quantified by QUANTI-Blue assay (Invivogen). In short, 20 μL of supernatant was transferred into 96-well plates along with 180 μL of QUANTI-Blue solution and incubated for 0.5 to 4 hours at room temperature. To determine SEAP levels, optical density (OD) of each well was read at 630 nm using a microplate spectrophotometer. Results were normalized by attributing 100% released SEAP levels to the positive controls, respectively, PAM2CSK4 for HEK Blue hTLR2 cells and S-LPS for HEK Blue hTLR4 and TDM cells, and expressed as mean of percentage ± standard error of the mean (SEM) of at least three independent experiments.

2.5. Cytokine Enzyme-Linked Immunosorbent Assay (ELISA)

Pro-inflammatory cytokine (TNF, IL-1β, and IL-6) levels were measured in supernatants after 3, 6 and 18 hours of exposure to compounds using the respective sensitive enzyme-linked immunosorbent assay (ELISA) kits (R&D Systems; #DY210-05, #DY201-05, #DY206-05). Supernatants were prepared with appropriate reagent diluent using the following dilution factors: TNF: S-LPS and FP20Rha 1:10, FP20 neat; IL-6: S-LPS and FP20Rha 1:2, FP20 neat; IL-1β: S-LPS, FP20Rha and FP20 1:2. Assays were performed following manufacturer's instructions using Nunc MaxiSorp 96 well flat-bottomed ELISA plates (Thermo Fisher Scientific). The optical density of each well was determined using a microplate reader set to 450 nm and wavelength correction was read at 570 nm.

2.6. Murine Immunization Experiments

C57BL/6 J mice were purchased from Charles River Laboratories (Lyon, France). Upon arrival, animals were maintained under 12 h light/dark cycles while receiving food and water ad libitum and were rested for 2 weeks prior to immunization. All procedures and experiments involving animals were approved by the Animal Research Ethics Board of CIC bioGUNE (P-CBG-CBBA-0922) and the Diputacion de Bizkaia as Competent Authority, according to the guidelines of the European Union Council (Directive 2010/63/EU) and Spanish Government regulations (RD 53/2013).

MPLA (InvivoGen) and FP20Rha were reconstituted in DMSO (Sigma-Aldrich) at a concentration of 1 mg/mL. EndoFit ovalbumin (OVA, InvivoGen) was utilized for immunizations. Inoculations were formulated with OVA (antigen), FP20Rha or MPLA (adjuvants) or PBS (vehicle), and PBS to achieve the appropriate dosages. Immunizations began at approximately 9 weeks of age. At day 0, mice received subcutaneous injections of 10 ug OVA with or without 10 μg of adjuvant. Mice were boosted with identical injections at day 21. Bleeding was performed the day before the first and second immunizations. At day 42, mice were euthanized by carbon dioxide followed by cervical dislocation, and blood was collected via intracardiac puncture. Blood collected in serum separator tubes (BD) was centrifuged at 125 × g for 5 min, and serum was stored at −80 °C until use.

Antibody responses were measured by capture ELISA. NUNC plates (Thermo Fisher Scientific) were coated overnight with 100 μL of coating buffer, containing 0.5 μg/mL OVA in 0.2 M sodium bicarbonate at pH 9.6. Following four washes with 200 μL of 0.05% Tween-PBS wash buffer in an automatic plate washer (BioTek), plates were blocked for 1 h with filtered 1% BSA-PBS assay diluent. Wells were aspirated, and serial dilutions (twofold) of the sera, starting at 1/100, were applied, followed by an incubation of 1 h. Horseradish peroxidase-conjugated goat anti-mouse secondary antibodies against IgG (Jackson ImmunoResearch), IgG1, IgG2b, IgG2c, and IgG3 (SouthernBiotech) were diluted 1:1000 in assay diluent. After six washes with a wash buffer, 100 μL of secondary antibody was added to each well for 45 min. Plates were washed eight times with 200

μL wash buffer, and then two times with 400 μL PBS. One hundred microliters of 3,3′,5,5′-tetramethylbenzidine peroxidase substrate solution (TMB, SeraCare) was added to each well and incubated for 30 min. After stopping the reaction with 100 μL of 2 M sulfuric acid, samples were measured with a microplate reader (BioTek Epoch) at 450 nm.

3. Supplementary References

[1] H.L. Casal, H.H. Mantsch, Polymorphic phase behaviour of phospholipid membranes studied by infrared spectroscopy, Biochim. Biophys. Acta 779 (1984) 381–401. https://doi.org/10.1016/0304-4157(84)90017-0.

[2] L.K. Tamm, S.A. Tatulian, Infrared spectroscopy of proteins and peptides in lipid bilayers, Q. Rev. Biophys. 30 (1997) 365–429. https://doi.org/10.1017/s0033583597003375.

[3] A. Barth, Infrared spectroscopy of proteins, Biochim. Biophys. Acta 1767 (2007) 1073–1101. https://doi.org/10.1016/j.bbabio.2007.06.004.

[4] E. Gazi, J. Dwyer, N.P. Lockyer, P. Gardner, J.H. Shanks, J. Roulson, C.A. Hart, N.W. Clarke, M.D. Brown, Biomolecular profiling of metastatic prostate cancer cells in bone marrow tissue using FTIR microspectroscopy: a pilot study, Anal. Bioanal. Chem. 387 (2007) 1621–1631. https://doi.org/10.1007/s00216-006-1093-y.

[5] M. Kacuráková, FT-IR study of plant cell wall model compounds: pectic polysaccharides and hemicelluloses, Carbohydr. Polym. 43 (2000) 195–203. https://doi.org/10.1016/s0144-8617(00)00151-x.

[6] S. Brézillon, V. Untereiner, L. Lovergne, I. Tadeo, R. Noguera, F.-X. Maquart, Y. Wegrowski, G.D. Sockalingum, Glycosaminoglycan profiling in different cell types using infrared spectroscopy and imaging, Anal. Bioanal. Chem. 406 (2014) 5795–5803. https://doi.org/10.1007/s00216-014-7994-2.

[7] H.T. Mohamed, V. Untereiner, G. Cinque, S.A. Ibrahim, M. Götte, N.Q. Nguyen, R. Rivet, G.D. Sockalingum, S. Brézillon, Infrared Microspectroscopy and Imaging Analysis of Inflammatory and Non-Inflammatory Breast Cancer Cells and Their GAG Secretome, Molecules 25 (2020). https://doi.org/10.3390/molecules25184300.

[8] D. Ami, P. Mereghetti, M. Leri, S. Giorgetti, A. Natalello, S.M. Doglia, M. Stefani, M. Bucciantini, A FTIR microspectroscopy study of the structural and biochemical perturbations induced by natively folded and aggregated transthyretin in HL-1 cardiomyocytes, Sci. Rep. 8 (2018) 12508. https://doi.org/10.1038/s41598-018-30995-5.

[9] P.T. Wong, R.K. Wong, T.A. Caputo, T.A. Godwin, B. Rigas, Infrared spectroscopy of exfoliated human cervical cells: evidence of extensive structural changes during carcinogenesis, Proc. Natl. Acad. Sci. U. S. A. 88 (1991) 10988–10992. https://doi.org/10.1073/pnas.88.24.10988.

[10] C. Kirschbaum, K. Greis, E. Mucha, L. Kain, S. Deng, A. Zappe, S. Gewinner, W. Schöllkopf, G. von Helden, G. Meijer, P.B. Savage, M. Marianski, L. Teyton, K. Pagel, Unravelling the structural complexity of glycolipids with cryogenic infrared spectroscopy, Nat. Commun. 12 (2021) 1201. https://doi.org/10.1038/s41467-021-21480-1.

[11] A. Derenne, K.-M. Derfoufi, B. Cowper, C. Delporte, E. Goormaghtigh, FTIR spectroscopy as an analytical tool to compare glycosylation in therapeutic monoclonal antibodies, Anal. Chim. Acta 1112 (2020) 62–71. https://doi.org/10.1016/j.aca.2020.03.038.

[12] M. Banyay, M. Sarkar, A. Gräslund, A library of IR bands of nucleic acids in solution, Biophys. Chem. 104 (2003) 477–488. https://doi.org/10.1016/s0301-4622(03)00035-8.

[13] A. Synytsya, J. Čopíková, P. Matějka, V. Machovič, Fourier transform Raman and infrared spectroscopy of pectins, Carbohydr. Polym. 54 (2003) 97–106. https://doi.org/10.1016/S0144-8617(03)00158-9.

[14] F. Cabassi, B. Casu, A.S. Perlin, Infrared absorption and raman scattering of sulfate groups of heparin and related glycosaminoglycans in aqueous solution, Carbohydr. Res. 63 (1978) 1–11. https://doi.org/10.1016/S0008-6215(00)80924-6.

[15] F. Parker, Applications of Infrared Spectroscopy in Biochemistry, Biology, and Medicine, Springer US, 2012. https://doi.org/10.1007/978-1-4684-1872-9.